Werner Götz
Thomas Gerber
Barbara Michel
Stefan Lossdörfer
Kai-Olaf Henkel
Friedhelm Heinemann

Immunohistochemical characterization of nanocrystalline hydroxyapatite silica gel (NanoBone®) osteogenesis: a study on biopsies from human jaws

Author's affiliations:
Werner Götz, Barbara Michel, Stefan Lossdörfer, Oral Biology Laboratory, Department of Orthodontics, University of Bonn, Dental Hospital, Bonn, Germany
Thomas Gerber, Department for Materials Research – Nanostructures, Institute for Physics, University of Rostock, Rostock, Germany
Kai-Olaf Henkel, Department of Oral and Maxillofacial Surgery, German Military Hospital Hamburg, Hamburg, Germany
Friedhelm Heinemann, Department of Prosthodontics, Gerontostomatology and Medical Material Sciences, University of Greifswald, Dental Hospital, Greifswald, Germany

Correspondence to:
Dr Prof. Werner Götz
Oral Biology Laboratory
Department of Orthodontics
University of Bonn
Dental Hospital
Welschnonnenstr. 17
D-53111 Bonn
Germany
Tel.: +49 0 228 287 22116
Fax: +49 0 228 287 22588
e-mail: wgoetz@uni-bonn.de

Date:
Accepted 28 December 2007

To cite this article:
Götz W, Gerber T, Michel B, Lossdörfer S, Henkel K-O, Heinemann F. Immunohistochemical characterization of nanocrystalline hydroxyapatite silica gel (NanoBone®) osteogenesis: a study on biopsies from human jaws. *Clin. Oral Impl. Res.* **19**, 2008; 1016–1026
doi: 10.1111/j.1600-0501.2008.01569.x

Key words: bone graft, hydroxyapatite, immunohistochemistry, osteoconduction, osteogenesis

Abstract

Objectives: Bone substitute biomaterials may be osteogenic, osteoconductive or osteoinductive. To test for these probable characteristics in a new nanoporous grafting material consisting of nanocrystalline hydroxyapatite embedded in a porous silica gel matrix (NanoBone®), applied in humans, we studied biopsies from 12 patients before dental implantation following various orofacial augmentation techniques with healing times of between 3.5 and 12 months.

Material and methods: Sections from decalcified specimens were investigated using histology, histochemistry [periodic acid Schiff, alcian blue staining and tartrate-resistant acid phosphatase (TRAP)] and immunohistochemistry, with markers for osteogenesis, bone remodelling, resorption and vessel walls (alkaline phosphatase, bone morphogenetic protein-2, collagen type I, ED1, osteocalcin, osteopontin, runx2 and Von-Willebrand factor).

Results: Histologically, four specific stages of graft transformation into lamellar bone could be characterized. During early stages of healing, bone matrix proteins were absorbed by NanoBone® granules, forming a proteinaceous matrix, which was invaded by small vessels and cells. We assume that the deposition of these molecules promotes early osteogenesis in and around NanoBone® and supports the concomitant degradation probably by osteoclast-like cells. TRAP-positive osteoclast-like cells were localized directly on the granular surfaces. Runx2-immunoreactive pre-osteoblasts, which are probably involved in direct osteogenesis forming woven bone that is later transformed into lamellar bone, were attracted. Graft resorption and bone apposition around the graft granules appear concomitantly.

Conclusions: We postulate that NanoBone® has osteoconductive and biomimetic properties and is integrated into the host's physiological bone turnover at a very early stage.

Autogenous bone has certain limitations to being thought of as a gold standard; thus, bone substitute and grafting biomaterials are becoming increasingly important for all aspects of surgery (for recent reviews, see Nather 2005; Sutherland & Bostrom 2005; Cutter & Mehrara 2006). Within the broad range of biomaterials used in craniofacial bone surgery (for a recent review, see Abukawa et al. 2006), bioceramics on the basis of calcium phosphate, e.g. hydroxyapatite (HA) or β-tricalciumphosphate (β-TCP) are the most widely used and considered to be biocompatible, non-immunogenic, osteoconductive and osteoinductive (for recent reviews, see Vikram et al. 2005; Abukawa et al. 2006; Ruhé et al. 2006). However, due to high-temperature sintering during the processing, the material density may be increased and the porosity decreased. These factors negatively influence osteoconductivity and resorption at the implantation site, and also such bioceramics may have a long degradation time and may even induce chronic inflammatory processes (for reviews, see Vikram et al. 2005; Abukawa

et al. 2006). New nanostructured materials could overcome these disadvantages. NanoBone® is a recently developed and approved granular material consisting of nanocrystalline HA embedded in a silica gel matrix (Gerike et al. 2006), which offers several of the advantages of nanostructural biomaterials (for a review, see Webster & Ahn 2006). Because of the open SiOH or SiO groups of polysilicic acid, the internal surface of this material is extremely large (about 84 m^2/g). The interconnecting pores in the silica gel have sizes ranging from 10 to 20 nm, leading to material porosity of about 60%. The surface of the granules is very rough, thus creating an interconnecting porous structure ranging from micrometer to millimeter dimensions. However, NanoBone® has a high breaking strength of about 40 Mpa (Gerber et al. 2000, 2003). Animal experiments using the minipig critical-size defect model showed a significant, higher rate of bone formation as compared with other HA and TCP materials or gelatine sponges and a nearly complete resorption 8 months after implantation (Henkel et al. 2005, 2006). The healing process in this model after 5 and 10 weeks was investigated histologically and immunohistochemically, revealing first insights into the cellular processes of osteogenesis (Gerber et al. 2006; Henkel et al. 2006; Rumpel et al. 2006). As a result of these animal experiments, of preliminary clinical data as well as of histological findings in bone biopsies taken after the implementation of the material, biological phenomena of osteoconduction, osteoinduction and early remodelling *in vivo* were postulated (Bienengräber et al. 2006; Gerber et al. 2006; Henkel et al. 2006). In this study, selected decalcified samples from NanoBone®-augmented human jaw bones were studied by means of histology, histochemistry and immunohistochemistry to investigate the biological phenomena anticipated. Immunohistochemically, common markers for osteogenesis and bone resorption were used to characterize ongoing cellular differentiation, matrix secretion, mineralization and remodelling. Some of these, namely runx2, alkaline phosphatase (AP), osteopontin (OP) and osteocalcin (OC), belong to the key phenotypic markers expressed in the osteogenic cell lineage (Heng et al. 2004; Franz-Odendaal et al. 2006). ED1 identifies cells of the mononuclear phagocyte family including osteoclasts (Dijikstra et al. 1985). The study does not focus on the quantitative extent of osteogenesis in correlation to clinical or patient data, but on the biological behavior of the substitute biomaterial and the general principles of osteogenesis and graft biodegradation.

Materials and methods

Materials

Twelve biopsies were taken by one of the authors (F. H.) and in various German private dental practices in correlation with implant placement. They originated from jaw bone sites augmented with NanoBone® (Artoss, Rostock, Germany; Dentaurum Implants, Ispringen, Germany) for two main indications (alveolar augmentation, sinus lift), but from different regions and after different healing time periods. Healing was evaluated clinically. Table 1 gives an overview of the samples used. NanoBone® was applied according to the manufacturer's instructions. Generally, NanoBone® granules were mixed with the patient's blood 1 : 1 until a sticky paste consistency was achieved. After variable time periods (Table 1), cylindric biopsies measuring about 2 mm in diameter and 10 mm in length were taken using hollow trephine burrs (Helmut Zepf, Seitingen-Oberflacht, Germany or Komet-Brasseler, Lemgo, Germany). Additionally, parasagittal sections of a sample taken from a mandible, surgically removed for tumor resection from a 65-year-old male patient, were used for immunohistochemical control. The sections were taken from tumor-free lateral borders of the specimen after histological evaluation. The study protocol was approved by the Ethics Committee of the University of Bonn and written informed consent was given by all patients.

Methods

Histology and histochemistry

All specimens were fixed by immersion in 4% buffered (Sörensen buffer) formaldehyde at room temperature (RT) for at least 1 day. They were then decalcified for 1 week in 4.1% disodium ethylenediamino tetraacetic acid solution, which was changed every 24 h. After hydration, tissues were dehydrated in an ascending series of ethanol and embedded in paraffin. Serial sagittal sections of 2–3 μm were cut. Selected sections were stained with hematoxylin–eosin (HE), azan, Masson–Goldner trichrome and periodic acid-Schiff (PAS) staining for histochemical detection of glycosaminoglycans and glycoproteins, respectively. In order to identify osteoclast-like cells, selected tissue sections were stained to demonstrate tartrate-resistant acid phosphatase (TRAP).

Immunohistochemistry

Selected sections from the median parts of the series were deparaffinized, rehydrated and rinsed for 10 min in tris-buffered saline

Table 1. **List of specimens investigated**

Case no.	Age of patient	Sex of patient	Indication	Region	Time after implementation (months)	Predominating stage of granule osteogenesis
1	34	Male	ap augmentation	24	3.5	I
2	27	Male	ap augmentation	25	4	I
3	72	Male	ap augmentation	21	3	II
4	55	Female	sinus lift	16	4	II
5	49	Male	Extraction, cystectomy, ap augmentation	21	5	II
6	35	Male	Sinus lift	16–17	5.5	II
7	62	Female	ap augmentation	13–14	6	II
8	40	Male	ap augmentation	21	4	III
9	69	Male	ap augmentation	31, 41–42	4	III
10	24	Male	Sinus lift	24–25	11	III
11	63	Male	Alveolar filling	12	4	IV
12	53	Male	ap augmentation	11	12	IV

ap, alveolar process. Stages of granule osteogenesis: I, mostly undegraded; II, mostly active remodelling: osteogenesis and resorption; III, mostly increased osteogenesis and remodeling, degraded granules; IV, ossification almost complete.

Table 2. **Primary antibody protocols**

Antibody	Isotype	Producer	Incubation protocol
Alkaline phosphatase (AP)	Rabbit polyclonal	Quartett (Berlin, Germany)	Ready to use, on, 4°C
BMP-2	Goat polyclonal	Santa Cruz (Santa Cruz, CA, USA)	1 : 25, on, 4°C
collagen type I	Mouse monoclonal	Abcam (Cambridge, UK)	1 : 200, 1 h, RT
ED1 (CD 68)	Mouse monoclonal	Dako (Glostrup, Denmark)	1 : 100, 1 h, RT
Osteocalcin (OC)	Mouse monoclonal	Takara (Otsu, Shiga, Japan)	1 : 100, 1 h, RT
Osteopontin (OP)	Rabbit polyclonal	Abcam	1 : 200, 1 h, RT
runx2	Goat polyclonal	Santa Cruz	1 : 30, on, 4°C
von-Willebrand factor (vWF)	Rabbit polyclonal	Linaris (Wertheim-Bettingen, Germany)	1 : 200, 1 h, RT

on, overnight; RT, room temperature.

(TBS). Endogenous peroxidase was blocked in a methanol/H_2O_2 (Merck, Darmstadt, Germany) solution for 45 min in the dark. After being rinsed, sections were pre-treated with PBS containing 1% bovine serum albumin for 20 min at RT and digested with 0.4% pepsin for 10 min at 37°C before collagen type I immunohistochemistry. Following further rinsings, sections were incubated with the primary antibodies in a humid chamber. For details and incubation protocols see Table 2. For the detection of mouse monoclonal antibody binding, sections were washed three times for 10 min in TBS and incubated with the peroxidase-conjugated EnVision™ anti-mouse system (Dako, Glostrup, Denmark) at RT for 30 min. For the detection of polyclonal rabbit and goat antibodies (see Table 2), EnVision™ anti-rabbit and anti-goat horse radish peroxidase-conjugated secondary antibody diluted 1 : 50 were applied for 30 min, respectively (both from Dako). Following a rinse, the peroxidase activity was visualized using diaminobenzidine, yielding a brown-staining product. Selected slides were counterstained with Mayer's hematoxylin.

Specificity controls were run by (i) omitting the primary antibody and incubating slides with TBS or normal horse serum instead and (ii) omitting primary antibodies or bridge and secondary antibodies, respectively. Positive controls were carried out using the mandibular specimens or fetal human bone tissues carrying known antigens.

A blind histological evaluation of all sections stained was undertaken by two investigators independently. A staging of osteogenesis of the single NanoBone® granules was established by investigating every biopsy section stained conventionally and histochemically (see 'Results'). Correlations between the staging of granule osteogenesis and clinical healing time, indications or patient data were not established and were beyond the scope of this study.

Immunohistochemical staining intensity was staged semiquantitatively (none, weak, moderate, strong and very strong immunostaining).

Results

Histology

The sections from the mandibular specimens showed age-related but normal bony and soft tissue structures. Focally, osteoblasts were found lying on the bone surfaces.

In the biopsies, due to the decalcification process, which leads to the dissolution of HA, NanoBone® aggregations or granules mostly appeared as amorphous, cloddy bodies of different sizes containing porous spaces ranging between 1 and 10 μm. The osteogenous transformation of the granules could be categorized into four different stages (I–IV) according to remodelling and bone formation, as described previously in minipig experiments (Gerber et al. 2006). Different stages of granule osteogenesis could be observed within the same specimen. The predominating stage of granule osteogenesis is indicated for every specimen in Table 1.

Stages of osteogenesis

Stage I. Non-degraded NanoBone® granules represented early stages of healing. They appeared porous (Figs 1–5) and were mostly covered by a dense connective tissue sheath (Fig. 1) containing fibroblast-like cells. Focally within the material, a few isolated cells or small cellular fibrovascular extensions as well as a few tubular structures resembling capillaries were cut as revealed by the analysis of serial sections. Loose, well-vascularized connective tissue occupied the areas between the grafted material (Fig. 2).

Stage II. More small tubular structures resembling vessels now penetrated the granules (Figs 3 and 4). Layers of osteoblast-like cells ensheathed the NanoBone® aggregations. At the interface, eosinophilic seams resembling osteoids as a sign of early desmal osteogenesis forming woven bone could be observed (Figs 2–5). With azan staining, they appeared blue, with Masson–Goldner staining green and both of these results indicated the occurrence of a collagenous matrix. Finger-like and interconnecting osteoid protrusions extended into the grafted material. These protrusions sometimes contained cells and small vessel-like structures (Fig. 4). As in stage I, single cells were cut within the material and, in most cases, they were surrounded by strands of connective tissue or by an osteoid-like matrix (Figs 3 and 4). Often, longish or cuboidal cells revealing osteoblasts covered the osteoid surfaces (Figs 2 and 5). In the developing bone tissue, osteoblasts were incorporated to become osteocytes (Fig. 4). Some of the woven bone trabeculae had increased in size and had become connected to bony structures from neighboring granules. Interfaces between the surface of the granules and newly formed bone were intensively stained in most cases. On the surface of the NanoBone® bodies as well as on newly formed bone, multinucleated osteoclast-like cells appeared. Typically, an osteoblastic and an osteoclastic compartment could be observed (Fig. 5).

Stage III. Increased material degradation and substitution by newly formed woven bone was seen. Typically, a bone-forming side with osteoblasts and an osteoid seam was opposite or next to a resorbing side consisting of graft material probably degraded by osteoclast-like cells. Smaller granules with no signs of bone formation

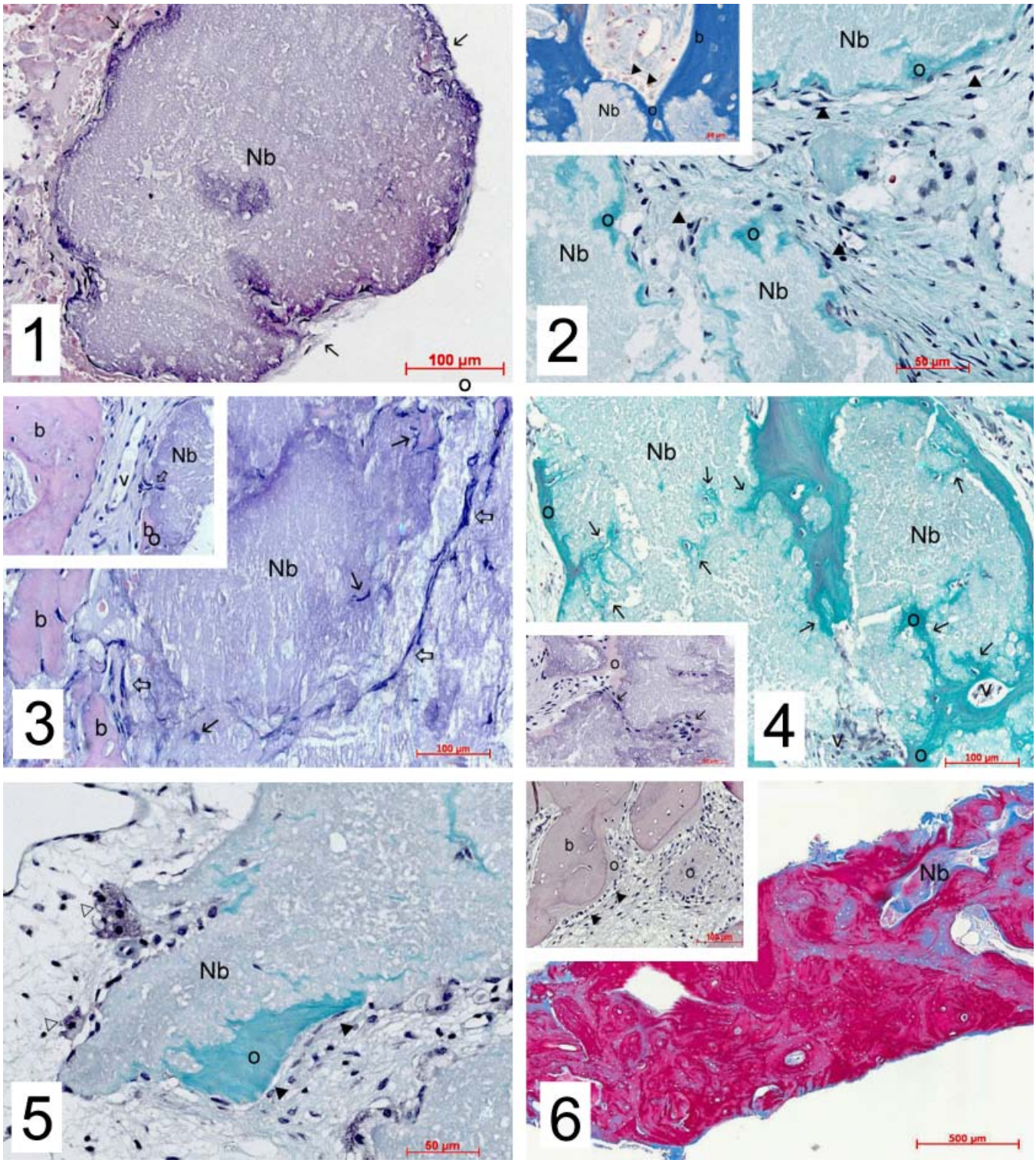

Fig. 1–6. (1) Case 1: non-degraded NanoBone® granule (Nb; stage I) covered by a connective tissue sheath (arrows). Hematoxylin–eosin staining, original magnification × 20. (2) Case 7: NanoBone® granules with early osteogenesis (Nb) covered by osteoblast (arrowheads), osteoid (o) deposition (stage II). Trichrome staining, × 40. Inset: Case 3: NanoBone® granules (Nb) with osteoid seam (o) and osteoblasts (arrowheads). b, newly formed bone trabeculae. Azan staining, × 40. (3) Case 3: granule (Nb; stage II) with invading vessel-like structures (open arrows) and single cells (arrows). b, newly formed bone at the periphery. Hematoxylin–eosin staining, × 40. Inset: same case: capillary-like structure (open arrow) invading granule (Nb), b, newly formed bone; v, vessel in intergranular connective tissue. Hematoxylin–eosin staining, × 40. (4) Same case as in Fig. 3. Osteoid (o) extensions (arrows) into NanoBone® granule (Nb). v, vessel-like structures. Trichrome staining, × 40. Inset: same case: fibrovascular extension (arrows) with osteoid deposition (right arrow), granule partly covered by osteoid (o). Hematoxylin–eosin staining, × 40. (5) Case 5: stage II granule (Nb), osteogenesis with newly formed osteoid (o), osteoblasts (arrow heads) and resorbing osteoclasts (open arrow heads). Trichrome staining, × 40. (6) Case 11: progressed osteogenesis (stage IV). Nb, NanoBone® residues within mature lamellar bone. Azan staining, × 5. Inset: Case 7: larger particle residues (Nb) beside newly formed, mineralized, lamellar bone (b). Azan staining, × 20. Inset: Case 12: progressed osteogenesis (stage IV), ongoing apposition of osteoid (o) on newly formed bone (b), arrowheads: osteoblasts. Hematoxylin–eosin staining, × 20.

were also attacked by such cells. During this remodelling phase, more tiny vessel-like structures originating from the intergranular connective tissue penetrated the material. Large areas of newly formed bone now appeared mineralized.

Stage IV. In the late stage of bone formation, residuals of woven bone were detectable within lamellar bone, indicating a previous remodelling (Fig. 6). Most biopsy specimens appeared to be nearly completely ossified (Fig. 6). The bone resembled a mature lamellar structure composed of osteons. Small residues of original NanoBone® material were sometimes visible within lamellar bone areas or within perforating or Haversian channels (Fig. 6). Sometimes, osteoid seams could also be observed (inset, Fig. 6).

In no specimen investigated were there any histological signs of inflammation, necrosis, debris or granuloma formation.

Histochemistry

PAS staining

A moderate PAS-positive staining was noted in the connective tissue among NanoBone® granules in all specimens investigated. Fibrous sheaths and their protrusions surrounding the granules were stained more intensively. A stronger PAS staining was observed for the whole or for larger areas of the NanoBone® granules belonging to stages I–II (Figs 7–9). Invasion of vessel-like structures was clearly visible (Fig. 9). Interfaces between granules and newly formed bone were also PAS-positive (Fig. 8). Newly formed bone focally appeared weak to moderately PAS positive for the bone matrix or for cement lines.

TRAP staining

Osteoclast-like cells in sections from all specimens investigated were TRAP stained. As a sign of early remodelling, TRAP-positive cells appeared at the surface of the NanoBone® granules as well as on the surfaces of newly formed bone spicules (Fig. 10). TRAP-positive mononuclear cells were also visible in the connective tissue, mainly around the vessels. TRAP-positive cells could also be found at the periphery of the granules, especially near vessel penetrations. In sections representing stages III and IV, the number of TRAP-positive cells decreased. However, on the surfaces of newly formed bone and around NanoBone® residues, osteoclast-like cells were still detectable.

Immunohistochemistry

AP

In the mandibular control section, some soft tissue areas, osteoblasts, focally some osteocytes and vessel walls were immunostained (data not shown).

Immunoreactive areas appeared mainly in the central parts of NanoBone® granules, in osteoblasts and as a weak staining at the interface between newly formed bone and the grafted material (Figs 11 and 12). Fibroblasts of the connective tissue were mainly unstained or weakly stained. However, fibroblasts close to granules also showed stronger imunoreactivity (Figs 11 and 12). In stage IV specimens, AP immunostaining also appeared weak in the matrix of the newly formed bone.

Bone morphogenetic protein-2 (BMP-2)

In the mandibular control section, only a few osteoblasts were stained (inset, Fig. 13).

Strong to very strong immunoreactive areas appeared mainly in more central parts of the grafts and at the interfaces along osteogenic fronts (Fig. 13). Large areas of the connective tissue were also immunoreactive, especially behind osteoblasts forming new bone (Fig. 14). In areas some distance away from grafted material or newly formed bone, immunostaining was weak or absent. In the newly formed bony structures, osteocytes and focal areas of the bone matrix were weakly stained (data not shown).

Collagen type I

In the mandibular bone section, collagen type I was found in osteoblasts, in a few osteocytes, weakly in the bone matrix and in all soft tissues (data not shown).

As for BMP-2, the NanoBone® matrix was stained intensively. Unfortunately, probably due to pepsin pre-digestion as a pre-requisite for immuohistochemistry, large central areas had been dissolved. In most cases, only the immunostained peripheral parts and the interfaces to newly formed bone were visible (Fig. 15). A stronger immunostaining was seen in the net-like osteoid protrusions (Fig. 15) and in osteoblasts. For the newly formed bone, collagen type I was found in the osteoid and later in the matrix of woven and lamellar bone as well as in osteocytes and osteoblasts (Fig. 16).

ED1

ED1 immunostaining resembled TRAP staining of macrophages and osteoclast-like cells in all specimens investigated. However, in contrast to the TRAP staining more mononuclear cells were labelled (Fig. 17).

OC

In the mandibular bone section, all osteocytes and osteoblasts were stained. Bone and soft tissue matrix were weakly immunostained (data not shown).

The matrix of nearly all NanoBone® granules showed strong to very strong immunoreactivity (Fig. 18); even smaller residues in stage IV specimens were immunostained. The strongest staining was seen in the peripheral parts of the granules and also along the interfaces between granules and newly formed bone (Fig. 19). Connective tissue was stained focally. Osteoblasts were immunoreactive (inset, Fig. 18). Newly formed osteoid matrix was not stained until it was mineralized. In the lamellar bone, the staining pattern was similar to the control bone, namely a weak to moderate reactivity of the bone matrix and a moderate to strong reaction in osteoblasts and osteocytes.

OP

In the mandibular bone section, osteoblasts and a few osteocytes were stained. In the bone matrix, cement lines appeared immunostained. Also, in the soft tissues, immunolabeling was visible (data not shown).

The immunoreactivity pattern in and around the granules was similar to that for OC, except for a stronger staining at the interfaces between granules and newly formed bone and within the connective tissue (Fig. 19). Newly formed bone in sections from stage III and IV biopsies was negative or showed weak focal immunostaining and staining in cement lines (inset, Fig. 19). Connective tissues in bony channels and also some osteoclast-like cells were immunostained (Fig. 19).

Runx2

In the mandibular bone section, only a few osteoblasts were stained weakly or moderately (data not shown).

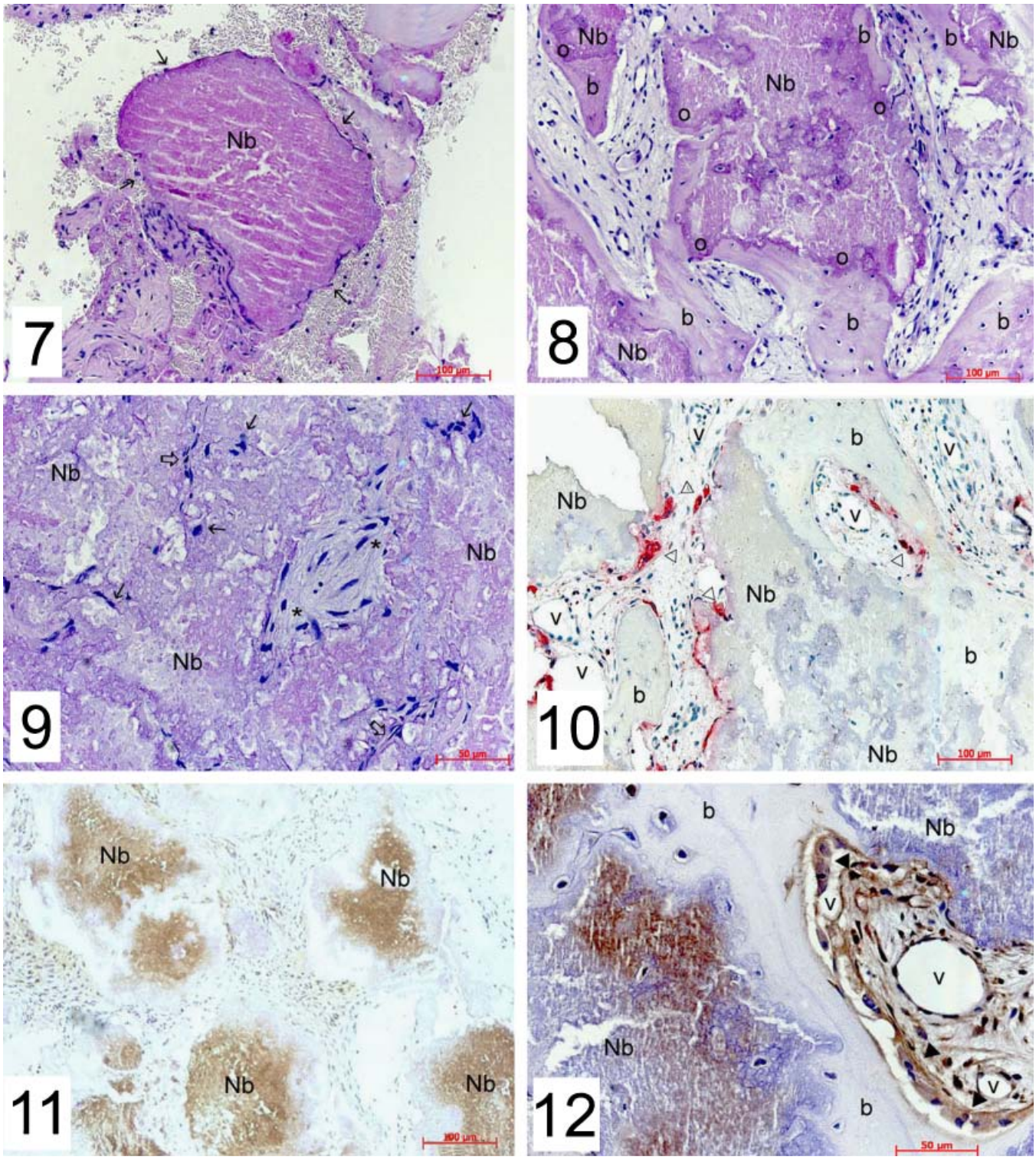

Fig. 7–12. (7) Case 1: non-degraded granule (Nb, stage I) with a thin connective tissue sheath (arrows), strong periodic acid Schiff (PAS) staining of the granule material. PAS, × 20. (8) Case 3: granule (Nb) with early osteogenesis (stage II). Strong periodic acid Schiff (PAS) staining along the interface between the granular matrix and the newly formed bone (b), strong staining of osteoid (o). PAS, × 20. (9) Case 7: non-degraded NanoBone® granule (Nb, stage I) with fibrovascular extension (asterisks), ingrown vessel-like structures (open arrows) and single cells (arrows). Periodic acid Schiff staining, × 40. (10) Case 3: osteoclasts (open arrow heads) around granule (Nb, stage II) and newly formed bone (b) surfaces. v, vessels. Tartrate-resistant acid phosphatase staining, × 20. (11) Case 7: alkaline phosphatase immunoreactivity in the central parts of granules (Nb, stage I). Diaminobenzidine, × 10. (12) Case 11: alkaline phosphatase immunoreactivity in NanoBone® (Nb) residue, in osteoblasts (arrowheads) and in fibroblasts of the connective tissue. v, vessels. Diaminobenzidine, × 40.

In the biopsy sections, runx2-immunoreactive cells were localized focally in connective tissue areas mainly around vessels. Also, some single cells cut within the NanoBone® material or within the osteoid extensions showed immunostaining (Fig. 20). Nearly all osteoblasts surrounding native and ossifying NanoBone® and on the surfaces of bony trabeculae were labelled

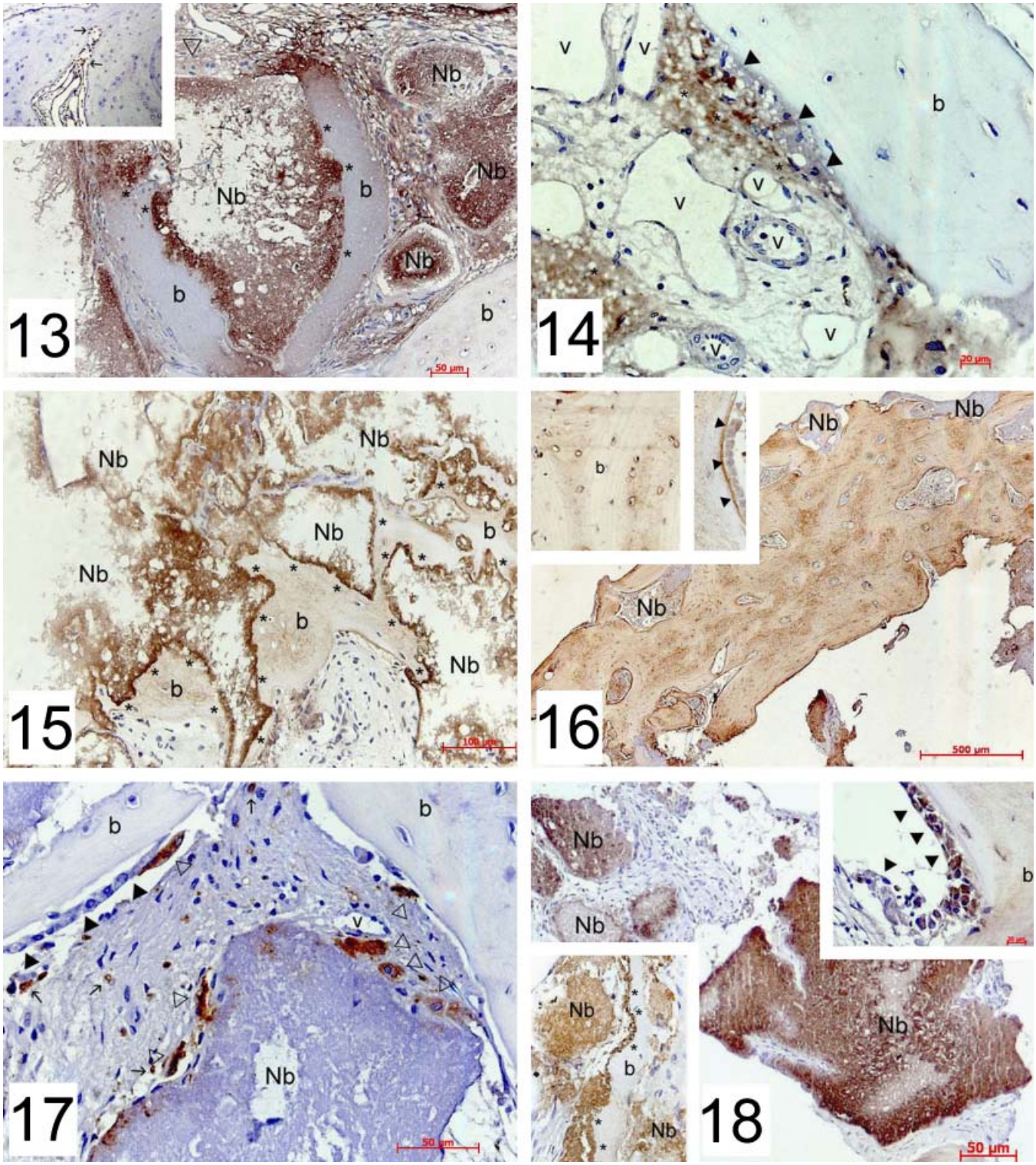

Fig. 13–18. (13) Case 10: strong bone morphogenetic protein (BMP)-2 immunoreactivity in the matrix of granules [Nb, stage I and II (right), III (left)]. b, newly formed bone. Diaminobenzidine (DAB), × 20. Inset: adult mandibular control specimen: weak to moderate BMP-2 immunostaining in some endosteal osteoblasts (arrows). DAB, × 20. (14) Same case as in Fig. 15. Bone morphogenetic protein-2 immunoreactivity in osteoblasts (arrowheads) and in the connective tissue behind them. v, vessels; b, newly formed bone. Diaminobenzidine, × 40. (15) Case 3: collagen type I immunostaining in the NanoBone® granules (Nb; stage II) and along the interfaces (asterisks) to newly formed bone (b). Diaminobenzidine, × 20. (16) Case 11: collagen type I immunostaining of newly formed, mature lamellar bone. Nb, NanoBone® residues. Diaminobenzidine (DAB), × 5. First inset on the left: Case 12: collagen type I immunoreactive osteocytes in newly formed bone (b). DAB, × 40. Second inset on the left: Case 9: collagen type I immunoreactive osteoid seam and osteoblasts (arrow heads) on newly formed bone. DAB, × 40. (17) Case 6: ED1 immunostaining of osteoclasts and mononuclear precursor cells (open arrowheads). Nb, NanoBone® granule (stage II); b, newly formed bone. Diaminobenzidine, × 40. (18) Same case as in Fig. 17. Osteocalcin (OC) immunostaining in NanoBone® granules (Nb). Diaminobenzidine, × 20. Right inset: same case: OC immunoreactive osteoblasts (arrowheads) along the surface of the newly formed bone (b). Diaminobenzidine (DAB), × 40. Left inset: Case 8: OC immunostaining in the granule matrix (Nb, stage II) and along the osteogenic interface (asterisks). b, newly formed bone. DAB, × 20.

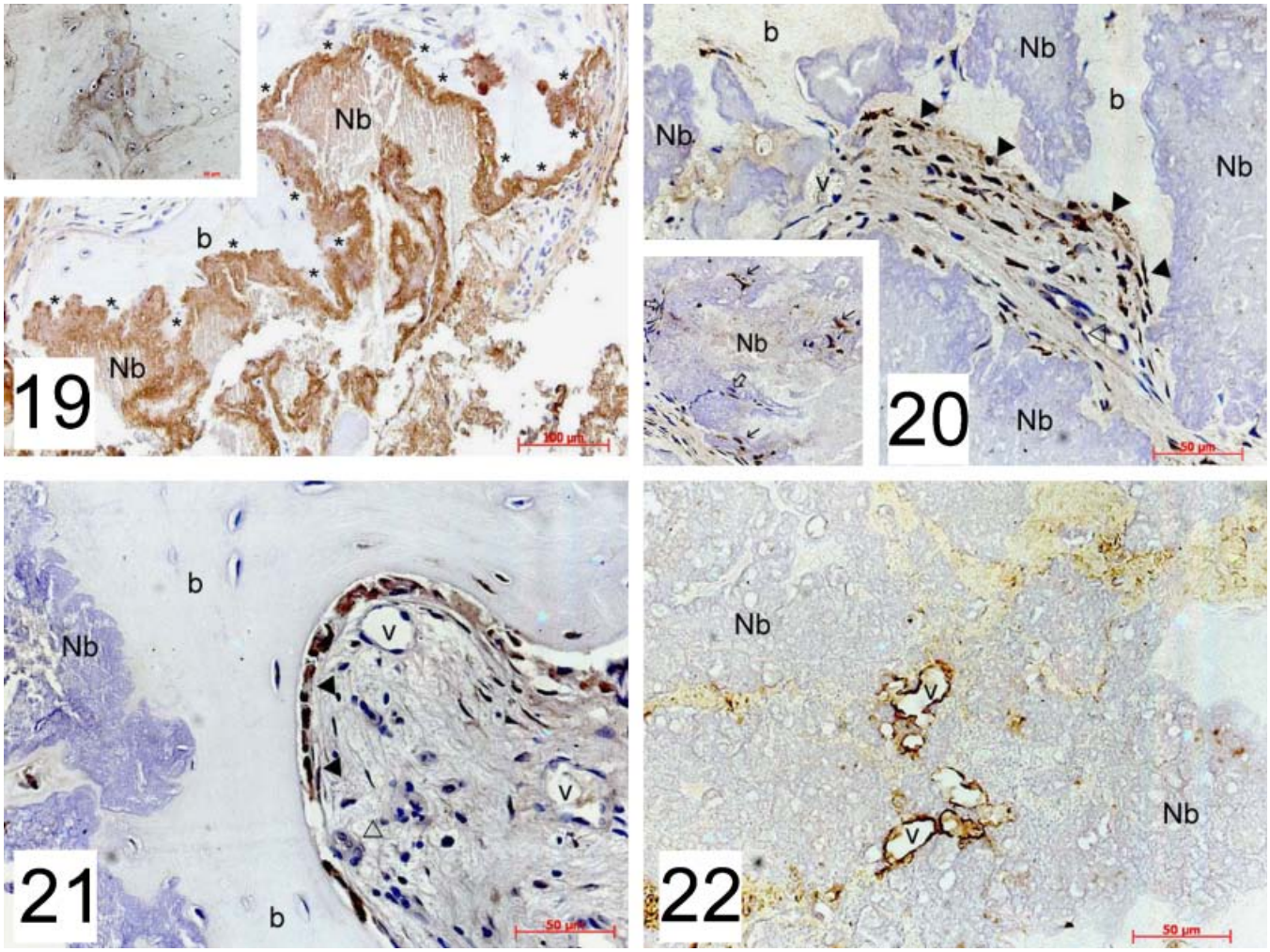

Fig. 19–22. (19) Case 11: osteopontin (OP) immunostaining along the osteogenic interface and in the osteoid (asterisks). Nb, NanoBone® granules (stage III–IV). Diaminobenzidine (DAB), × 10. Inset: Case 12: focal OP immunostaining in the bone matrix and in the cement lines. DAB, × 40. (20) Case 7: runx2 immunostaining in osteoblasts (arrowheads) and pre-osteoblasts in the connective tissue behind them. b, newly formed bone; Nb, NanoBone® granules (stage I). Diaminobenzidine (DAB), × 40. Inset: same case: runx2 immunoreactive cells near invading vessels (open arrow) and within NanoBone® granule (Nb). DAB, × 20. (21) Case 11: runx2 immunoreactive osteoblasts (arrowheads) along the surface of the newly formed, mature bone (b). v, vessels; Nb, NanoBone® granules; open arrowhead, unstained osteoclast. Diaminobenzidine, × 40. (22) Case 6: Von-Willebrand factor-immunostained walls of small vessels (v) sectioned with a NanoBone® granule (Nb). Diaminobenzidine, × 40.

(Fig. 21). The number of runx2-positive osteoblasts lying on bone surfaces had decreased in sections containing stage III or IV granules.

Von-Willebrand factor (vWF)

In all sections investigated, walls of the vessel-like structures were stained. Small vessels within granules or penetrating granules could be clearly identified in stage II or later-staged specimens (Fig. 22).

Immunostaining controls

No immunoreactivity was observed in any of the immunohistochemically negative control specimens.

Discussion

The behavior of bone substitute materials in animal experiments and from grafted sites in humans can be investigated by conventional histological staining that includes a variety of standard methods (Gedrange et al. 2006). These provide information on the microstructure of the graft with respect to integration or osteogenesis, but not on the factors involved in these processes. Immunohistochemical techniques allow the detection of molecules that are involved in osteoblast differentiation, bone mineralization or remodelling. To date, only a few studies on bone graft healing in humans, using immunohistochemistry, have been published (Tapety et al. 2004; Zerbo et al. 2005). In this study, histochemical and immunohistochemical methods were applied to study graft osteogenesis in 12 human specimens after implantation of a new highly porous nanocrystalline HA (NanoBone®).

The histological analysis revealed certain phenomena of bone formation and remodelling in and around the NanoBone® granules, which we characterized chronologically as a sequence of material transformation from stage I to IV representing ongoing osteogenesis and remodelling. Granules representing stage I were mainly intact and non-degraded. The intergranular space was filled with connective tissue.

Histologically, the granules consisted of an amorphous matrix, reflecting the macroporous and microporous structures of the graft material (Gerber et al. 2006). Because HA is lost due to decalcification during the histotechnical process, this matrix should consist mainly of organic material. It is known from recent investigations by scanning electron microscopy and energy-dispersive X-ray analysis that the SiO_2 gel matrix of NanoBone® is degraded after a short implantation time and substituted for by an unstructured organic matrix (Gerber et al. 2006). Indeed, the positive PAS reaction within the material indicated the presence of glycoproteins. PAS staining correlated with a moderate to strong immunostaining for most of the proteins investigated (AP, BMP-2, collagen type I, OC and OP). Therefore, we presume that bone-specific proteins and growth factors, such as BMP-2, were absorbed during the early months of graft healing. Probably SiO_2 was substituted for by these organic factors. Blood serum, in which numerous soluble proteins and a wealth of growth factors are carried, may be a probable source after destruction of small blood vessels during the surgical procedures in the host region, because the proteins investigated in this study all occur not only in the bone matrix but also in the serum (Flohr et al. 2003). However, it cannot be excluded that, after implantation of the graft material, local cells could have secreted these molecules. Because the immunostaining for AP and BMP-2 was concentrated in the center of the granules, it can be supposed that these factors may have been incorporated at an earlier time than OC or OP, which were localized at the periphery of the material. Thus, the nanoporosity of NanoBone® had allowed the circulation of body fluids and the influx, adherence or incorporation of proteins to establish a proteinaceous organic matrix. Immobilization and absorption of proteins to implant and graft materials is a well-known phenomenon (Ruhé et al. 2006; Webster & Ahn 2006) and fluid flow and diffusion of proteins have been discussed for various bioceramics, e.g. TCP (Zerbo et al. 2001; Vikram et al. 2005), but never demonstrated immunohistochemically for human specimens as in our study. Implantation experiments using NanoBone® in the critical-size defect model in minipigs have revealed similar findings (Gerber et al. 2006). This matrix, enriched with bioactive factors and thus mimicking physiological bone extracellular matrix, now serves as an osteoinductive focus by triggering osteogenesis. All of the bone matrix proteins detected are able to attract, adhere and promote differentiation of osteoblast precursor cells (for reviews, see Young 2003; McKee et al. 2005). The presence of collagen type I, as shown from our immunohistochemical data, is also considered an important prerequisite for the attachment of osteoblasts to biomaterial surfaces (Cowan et al. 2005). BMP-2 as a potent osteogenic factor is a promotor of bone formation and osteoblast differentiation and regulates the bone-specific proteins investigated in this study (for a recent review, see Derner & Anderson 2005). The strong immunostaining for BMP-2 points to an important role during the early steps of NanoBone® transformation. In control sections from adult jaw bone, BMP-2 was only detectable in some of the osteoblasts. Our data show that the implantation of NanoBone® has led to a strong immunostaining of BMP-2 in the host region. BMP-2 expression was detected after the implementation of collagen lyophilisate or autogenous bone in a critical-size defect model of the pig (Thorwarth et al. 2005), but to our knowledge never described in humans. However, this probable effect of NanoBone® on the induction of endogenous BMP-2 needs further investigation.

From *in vitro* studies, it is known that osteogenic cells show good attachment, differentiation or migration on various ceramic surfaces (Blokhuis et al. 2000). This is also the case for NanoBone®. In sections containing stage I granules, these were covered by a thin connective tissue sheath containing a layer of cells, which, according to their structure and their immunohistochemical staining pattern, can be classified as pre-osteoblasts. The nature of these cells was especially confirmed by immunostaining for runx2, which is a marker for immature osteoblasts and essential for osteoblast differentiation (for a review, see Schroeder et al. 2005). Runx2-positive cells were also detected in the connective tissue between the graft granules, especially around the vessels. This shows that osteoblast progenitor cells may originate from the connective tissue or from the perivascular areas in the grafted areas and documents the fact that immature cells are recruited and stimulated to develop into osteoblasts. Therefore, NanoBone® may have osteoinductive properties according to common definitions (Albrektsson & Johansson 2001). However, implantation studies will be necessary to check this assumption and to prove ectopic bone formation. Further findings from the analysis of serial sections showed that not only are peripheral osteoblasts involved in osteogenesis but that some single cells or cells embedded in fibrovascular strands could also be found inside the granules. Some of these cells showed positive immunostaining for runx2 and for AP, the latter being a marker for more mature osteoblasts (Bonucci & Nanci 2001). Obviously, pre-osteoblastic 'pioneer' cells were able to penetrate the graft matrix or had been transported by ingrowing vessels into the interior. Recently, runx2-positive cells have also been found during osteogenesis within TCP grafts (Zerbo et al. 2005). According to our histological data, capillary invasion into NanoBone® already occurred very early. Staining with vWF revealed the existence of a network of small vessels within some granules. Whether the porous structure of a biomaterial and the metabolic environment within it allow and promote cell and vessel invasion has to be proven for NanoBone® in further studies.

Around and within stage II granules, direct or desmal osteogenesis appeared. According to the morphology, osteoid-like seams sometimes covered by osteoblasts appeared. The osteoid front shows a very close proximity to the NanoBone® matrix, indicating a direct interaction. Immunohistochemistry again could detect some of the bone matrix proteins investigated in osteoblasts and osteoid. Generally, the detection of AP, collagen type I, OC and OP during these early osteogensis processes in and around NanoBone® corresponds to their occurrence and function during physiological osteogenesis (Cowles et al. 1998; Bonucci & Nanci 2001; Young 2003; Standal et al. 2004; Alford & Hankenson 2006). BMP-2 as an osteogenic growth factor was still found along the osteogenic front line and also in the connective tissue behind the osteoblasts. The ossification of the osteoid matrix occurred at multiple sites within

the newly formed bone trabeculae and could clearly be diagnosed by the conventional histological staining used. Also, immunostaining for bone matrix proteins e.g., collagen type I or OC increased during mineralization. The correlation of these proteins with osteoid mineralization is a well-known phenomenon in normal osteogenesis (Cowles et al. 1998; Young 2003) and strengthens the view that osteogenesis around and in NanoBone® mimics physiological phenomena. With ongoing osteogenesis, interconnecting osteoid protrusions and extension into the NanoBone® granules were seen. Probably isolated foci of osteogenesis also appear around the 'pioneer' cells in the interior of the granules.

Interestingly, the interface between granules and newly formed osteoid or mineralized bone was stained intensively in the histological and PAS stainings and also immunohistochemically for some of the components investigated, e.g. OP. This zone could be interpreted as a form of adhesion or cement line and may be compared with cement lines occurring in lamellar bone or tooth cementum, which are also characterized by the accumulation of specific matrix proteins such as OP (McKee et al. 2005).

A fast degradation by cellular resorption or chemical dissolution and a subsequent bony substitution at the same time is an important condition for the quality of bone graft biomaterials, which is not realized for most of the bone substitute ceramics (Abukawa et al. 2006). For example, for TCP, the data on resorption are conflicting. Whereas a paucity of resorbing cells and a slow degradation or resorption are complained about in some studies (Handschel et al. 2002; Zerbo et al. 2005; Suba et al. 2006), in other studies almost complete resorption is noted (Horch et al. 2006). However, degradation characteristics may differ among different forms of TCP. β-TCP, the low-temperature modification of TCP, for example, may show accelerated degradation in contrast to α-TCP, the high-temperature modification (Wiltfang et al. 2002). In the case of the material studied here, no delayed resorption was observed. According to recent findings in animal experiments (Gerber et al. 2006; Rumpel et al. 2006), multinucleated TRAP-positive osteoclast-like cells were identified. The immunohistochemical investigations using the ED1 antibody, which is a marker for cells of the mononuclear phagocyte family including clastic cells (Dijikstra et al. 1985), showed that macrophages as osteoclast precursors appeared around vessels and within the connective tissue between the graft granules. The osteoclast-like cells were not only localized along the surface of the newly formed bone but also directly on the NanoBone® granules. However, from the light microscopical findings, it was not clear whether these cells were in an active resorbing or an inactive state. For example, further ultrastructural investigations are needed in order to look for ruffled borders. If these cells are involved in the material resorption, this would facilitate a replacement of the graft to make space for the concomitantly occurring osteogenesis. In later stages, a compartmentalization was obvious due to the observation of a side with TRAP-positive cells and an osteogenic side with osteoblasts around the same NanoBone® granule. This demonstrates the integration of the bone-grafting material into the physiological remodelling processes of the human host. The reasons why osteoclast-like cells prefer to settle on the graft material must be discussed against the background of the already described proteinaceous character mimicking bone matrix. OP as well as OC, which have both been immunohistochemically detected in the matrix, play a role in the adhesion and differentiation of osteoclasts (Young 2003; Standal et al. 2004). Especially, OP promotes osteoclast adhesion and resorption (McKee & Nanci 1996; Asou et al. 2001). Furthermore, osteoclasts are able to synthesize OP (Alford & Hankenson 2006) and, therefore, appear to be immunoreactive in some sections. Additionally, *in vitro* studies have shown that osteoclast functions are increased on the surface of nanostructured biomaterials (Webster & Ahn 2006). Inflammatory processes have never been observed in the specimens investigated. Chronic inflammation and granuloma formation accompanying biodegradation are known phenomena following application of sintered ceramics and may impede osteogenesis (Koerten & van der Meulen 1999). Only very few and small remnants of NanoBone® were seen in osteogenesis stage IV specimens. In contrast, some of the other biomaterials, e.g. bovine HA, take several years to be resorbed (Taylor et al. 2002).

Granules in later osteogenesis (stage III) were covered by increasing areas of newly formed bone. All bony trabeculae were shown to be involved in remodelling processes, as revealed by further active osteogenesis seen by the deposition of osteoid seams by osteoblast layers and by resorptive activities as seen by TRAP-positive and ED1-positive osteoclasts lying within resorption lacunae. Additionally, the transformation of woven into mature lamellar bone took place. The fully developed mature bone as seen in sections containing stage IV granules consists of lamellar bone containing dispersed residues of woven bone. Its immunostaining pattern, e.g. for OP or OC was similar to the pattern observed in the adult control bone and described in the literature (McKee et al. 2005), indicating that it had reached full maturity.

Acknowledgements: We would like to thank Mrs I. Bay for technical assistance, Mrs C. Maelicke-Cole, BSc, for editing the manuscript and the following private dental practices (all in Germany) for providing the specimens: Drs Heinze (Berlin), Hoffmann and Puschmann (Jena), Hotz (Sigmaringen), Klingler (Bad Salzungen), Scopp (Berlin) and Sontheimer and Fries (Issing).

References

Abukawa, H., Papadaki, M., Abulikemu, M., Leaf, J., Vacanti, J.P., Kaban, L.B. & Troulis, M.J. (2006) The engineering of craniofacial tissues in the laboratory: a review of biomaterials for scaffolds and implant coatings. *Dental Clinics of North America* **50**: 205–216.

Albrektsson, T. & Johansson, C. (2001) Osteoinduction, osteoconduction and osseointegration. *European Spine Journal* **10**: S96–S101.

Alford, A.I. & Hankenson, K.D. (2006) Matricellular proteins: extracellular modulators of bone development, remodeling, and regeneration. *Bone* **38**: 749–757.

Asou, Y., Rittling, S.R., Yoshitake, H., Tsuji, K., Shinomiya, K., Nifuji, A., Denhardt, D.T. & Noda, M. (2001) Osteopontin facilitates angiogenesis, accumulation of osteoclasts, and resorption in ectopic bone. *Endocrinology* **142**: 1325–1332.

Bienengräber, V., Gerber, T., Henkel, K.O., Bayerlein, T., Proff, P. & Gedrange, T. (2006) The clinical application of a new synthetic bone grafting material in oral and maxillofacial surgery. *Folia Morphologica (Warszaw)* **65**: 84–88.

Blokhuis, T.J., Termaat, M.F., den Boer, F.C., Patka, P., Bakker, F.C. & Haarman, J.T.M. (2000) Properties of calcium phosphate ceramics in relation to their *in vivo* behavior. *The Journal of Trauma: Injury, Infection and Critical Care* **48**: 179–186.

Bonucci, E. & Nanci, A. (2001) Alkaline phosphatase and tartrate-resistant acid phosphatase in osteoblasts of normal and pathologic bone. *Italian Journal of Anatomy and Embryology* **106** (Suppl. 1): 129–133.

Cowan, M.C., Soo, C., Ting, K. & Wu, B. (2005) Evolving concepts in bone tissue engineering. *Current Topics in Developmental Biology* **66**: 239–285.

Cowles, E.A., DeRome, M.E., Pastizzo, G., Brailey, L.L. & Gronowicz, G.A. (1998) Mineralization and the expression of matrix proteins during *in vivo* bone development. *Calcified Tissue International* **62**: 74–82.

Cutter, C.S. & Mehrara, B.J. (2006) Bone grafts and substitutes. *Journal of Long Term Effects of Medical Implants* **16**: 249–260.

Derner, R. & Anderson, A.C. (2005) The bone morphogenetic protein. *Clinics in Podiatric Medicine and Surgery* **22**: 607–618.

Dijikstra, C.D., Döpp, E.A., Joling, P. & Kraal, G. (1985) The heterogeneity of mononuclear phagocytes in lymphoid organs: distinct macrophage subpopulations in the rat recognized by monoclonal antibodies ED1, ED2 and ED3. *Immunology* **54**: 589–599.

Flohr, B., Woitge, H.W. & Seibel, M.J. (2003) Molecular markers of bone turnover. Basic and analytical aspects. In: Orwoll, E.S. & Biliziotes, M., eds. *Osteoporosis: Pathophysiology and Clinical Management (Contemporary Endocrinology)*, 163–184. Totowa: Humana Press.

Franz-Odendaal, T.A., Hall, B.K. & Witten, P.E. (2006) Buried alive: how osteoblasts become osteocytes. *Developmental Dynamics* **235**: 176–190.

Gedrange, T., Bayerlein, T., Fanghänel, J., Landsberger, P., Hoffmann, A., Kauschke, E., Rumpel, E., Gerike, W., Bienengräber, V. & Proff, P. (2006) Critical considerations on the diagnostic appraisal, adaptation and remodelling of bone graft substitutes. *Folia Morphologica (Warszaw)* **65**: 59–62.

Gerber, T., Holzhüter, G., Götz, W., Bienengräber, V., Henkel, K.-O. & Rumpel, E. (2006) Nanostructuring of biomaterials – a pathway to bone grafting substitute. *European Journal of Trauma* **32**: 132–140.

Gerber, T., Holzhüter, G., Knoblich, B., Dörfling, P., Bienengräber, V. & Henkel, K.-O. (2000) Development of bioactive sol–gel material template for *in vitro* and *in vivo* synthesis of bone material. *Journal of Sol–Gel Science Technology* **19**: 441–445.

Gerber, T., Traykova, T., Henkel, K.-O. & Bienengräber, V. (2003) Development and *in vivo* test of sol–gel derived bone grafting materials. *Journal of Sol–Gel Science Technology* **26**: 1173–1178.

Gerike, W., Bienengräber, V., Henkel, K.-O., Bayerlein, T., Proff, P., Gedrange, T. & Gerber, T. (2006) The manufacture of synthetic non-sintered and degradable bone grafting substitutes. *Folia Morphologica (Warszaw)* **65**: 54–55.

Handschel, J., Wiesmann, H.P., Stratmann, U., Kleinheinz, J., Meyer, J. & Joss, U. (2002) TCP is hardly resorbed and not osteoconductive in a non-loading calvarial model. *Biomaterials* **23**: 1689–1695.

Heng, B.C., Cao, T., Stanton, L.W., Robson, P. & Olsen, B. (2004) Strategies for directing the differentiation of stem cells into the osteogenic lineage *in vitro*. *Journal of Bone and Mineral Research* **19**: 1379–1394.

Henkel, K.-O., Gerber, T., Dörfling, P., Gundlach, K.K.H. & Bienengräber, V. (2005) Repair of bone defects by applying biomatrices with and without autologous osteoblasts. *Journal of Cranio-Maxillofacial Surgery* **33**: 45–49.

Henkel, K.-O., Gerber, T., Lenz, S., Gundlach, K.K.H. & Bienengräber, V. (2006) Macroscopical, histological, and morphometric studies of porous bone-replacement materials in minipigs 8 months after implantation. *Oral Surgery, Oral Medicine, Oral Pathology, Oral Radiology and Endodontology* **102**: 606–613.

Horch, H.-H., Sader, R., Pautke, C., Neff, A., Deppe, H. & Kolk, A. (2006) Synthetic, pure-phase beta-tricalcium phosphate ceramic granules (Cerasorb®) for bone regeneration in the reconstructive surgery of the jaws. *International Journal of Oral and Maxillofacial Surgery* **35**: 708–713.

Koerten, H.K. & van der Meulen, J. (1999) Degradation of calcium phosphate ceramics. *Journal of Biomedical Materials Research* **44**: 78–86.

McKee, M.D., Addison, W.N. & Kaartinen, M.T. (2005) Hierarchies of extracellular matrix and mineral organization in bone of the craniofacial complex and skeleton. *Cells Tissues Organs* **181**: 176–188.

McKee, M.D. & Nanci, .A. (1996) Osteopontin at mineralised tissue interfaces in bone, teeth, and osseointegrated implants: ultrastructural distribution and implications for mineralised tissue formation, turnover, and repair. *Microscopy Research and Technique* **33**: 141–164.

Nather, A., ed. (2005) *Bone Grafts and Bone Substitutes. Basic Science and Clinical Applications*. New Jersey: World Scientific.

Ruhé, P.Q., Wolke, J.G.C., Spauwen, P.H.M. & Jansen, J.A. (2006) Calcium phosphate ceramics for bone tissue engineering. In: Bronzino, J.D., ed. *Tissue Engineering and Artificial Organs (The Biomedical Engineering Handbook)*. 3rd edition, 38-1–38-18. Boca Raton: Taylor & Francis.

Rumpel, E., Wolf, E., Kauschke, E., Bienengräber, V., Bayerlein, T., Gedrange, T. & Proff, P. (2006) The biodegradation of hydroxyapatite bone graft substitutes *in vivo*. *Folia Morphologica (Warszaw)* **65**: 43–48.

Schroeder, T.M., Jensen, E.D. & Westendorf, J.J. (2005) Runx2: a master organizer of gene transcription in developing and maturing osteoblasts. *Birth Defects Research Part C: Embryo Today, Reviews* **75**: 213–225.

Standal, T., Borset, M. & Sundan, A. (2004) Role of osteopontin in adhesion, migration, cell survival and bone remodelling. *Experimental Oncology* **26**: 179–184.

Suba, Z., Takás, D., Matusovits, D., Barabás, J., Fazekas, A. & Szabó, G. (2006) Maxillary sinus floor grafting with ß-tricalcium phosphate in humans: density and microarchitecture of the newly formed bone. *Clinical Oral Implants Research* **17**: 102–108.

Sutherland, D. & Bostrom, M. (2005) Grafts and bone graft substitutes. In: Liebermann, J.R. & Friedlaender, G.E., eds. *Bone Regeneration and Repair. Biology and Clinical Application*, 133–156. Totowa: Humana Press.

Tapety, F.I., Amizuka, N., Uoshima, K., Nomura, S. & Maeda, T. (2004) A histological evaluation of the involvement of Bio-Oss in osteoblastic differentiation and matrix synthesis. *Clinical Oral Implants Research* **15**: 315–324.

Taylor, J.C., Cuff, S.E., Leger, J.P.L., Morra, A. & Anderson, G.I. (2002) *In vitro* osteoclast resorption of bone substitute biomaterials used for implant site augmentation: a pilot study. *International Journal of Oral & Maxillofacial Implants* **17**: 321–330.

Thorwarth, M., Rupprecht, S., Falk, S., Felszeghy, E., Wiltfang, J. & Schlegel, K.A. (2005) Expression of matrix proteins during de novo bone formation using a bovine collagen and platelet-rich plasma (prp) – an immunohistochemical study. *Biomaterials* **26**: 2575–2584.

Vikram, D., Nather, A. & Khalid, K.A. (2005) Role of ceramics as bone graft substitutes. In: Nather, A., ed. *Bone Grafts and Bone Substitutes. Basic Science and Clinical Applications*, 445–458. New Jersey: World Scientific.

Webster, T.J. & Ahn, E.S. (2006) Nanostructured biomaterials for tissue engineering bone. *Advances in Biochemical Engineering, Biotechnology* **103**: 275–308.

Wiltfang, J., Merten, H.A., Schlegel, K.A., Schultze-Mosgau, S., Kloss, F.R., Rupprecht, S. & Kessler, P. (2002) Degradation characteristics of α and ß tri-calcium-phosphate (TCP) in minipigs. *Journal of Biomedical Materials Research (Applied Biomaterials)* **63**: 115–121.

Young, M.F. (2003) Bone matrix proteins: their function, regulation, and relationship to osteoporosis. *Osteoporosis International* **14** (Suppl. 3): S35–S42.

Zerbo, I.R., Bronckers, A.L., de Lange, G. & Burger, E.H. (2005) Localisation of osteogenic and osteoclastic cells in porous beta-tricalcium phosphate particles used for human maxillary sinus floor elevation. *Biomaterials* **26**: 1445–1451.

Zerbo, I.R., Bronckers, A.L.J.J., de Lange, G.L., van Beek, G.J. & Burger, E.H. (2001) Histology of human alveolar bone regeneration with a porous tricalcium phosphate. A report of two cases. *Clinical Oral Implants Research* **12**: 372–378.

